
CHAPTER 2

EXPERIMENTAL

2.1.0 Introduction

In this chapter we have presented the synthesis procedure for growing polypyrrole nanotubes and gold-polypyrrole composite . In order to find the composition we have used several characteristic techniques like Scanning electron microscopy, Transmission microscopy, Energy dispersive x-ray spectroscopy, Secondary ion-mass spectroscopy. We have also presented techniques using which we have made electrical contacts (single as well as multiple nanotubes) from these nanotubes for electrical transport measurements. The details of our instrumentation for low temperature measurements and characterization techniques are also described here.

2.2.0 Synthesis of nanowires

Synthesis of nanomaterials has been done mainly in two ways (1) Top-down and (2) bottom up method. In top-down method, a nano-dimension object is obtained by milling or plastic deformation down a macroscopic object. Control over the shape and size of the nano-object is not good in this process. In bottom-up process, few atoms or molecules assemble together driven by some chemical forces to form a nano-structure of well defined shape and size. Template based synthesis is one of the popular bottom-up technique of nanostructure fabrication. Depending on the requirements and material properties, different types of template have been used such as Stepped substrate [87], Grooved substrate [88], Self-assembly using organic surfactant or block copolymer [89], biological macromolecules such as DNA or rod shaped viruses [90–93], porous membranes/materials [94, 95] etc. The main merits of template based synthesis are (a) fine control on the shape and size, (b) easy processing, (c) high yield (d) cost-effectiveness and (e) doping control. Template based synthesis technique [94] is a high yield and low cost method for fabricating nanowires of desired size and high aspect ratio. We have synthesized nanowires of conducting polymers (Polypyrrole and Polyaniline) using this technique by chemical process. We have taken Polycarbonate membrane of various pore diameters ranging from 10 nm to 200 nm as template and thickness from 6 μm to 20 μm . Pore density in Polycarbonate membrane ranges from $\sim 10^6$ to 10^9 pores cm^{-2} depending on the pore diameter. The pores of the polycarbonate membrane, were prepared by track-etch method [96, 97] where a polymeric sheet of few micron thickness is bombarded with energetic ($\sim \text{MeV}$) heavy ions that leads to linear narrow path of radiation damage called track. The tracks can be re-

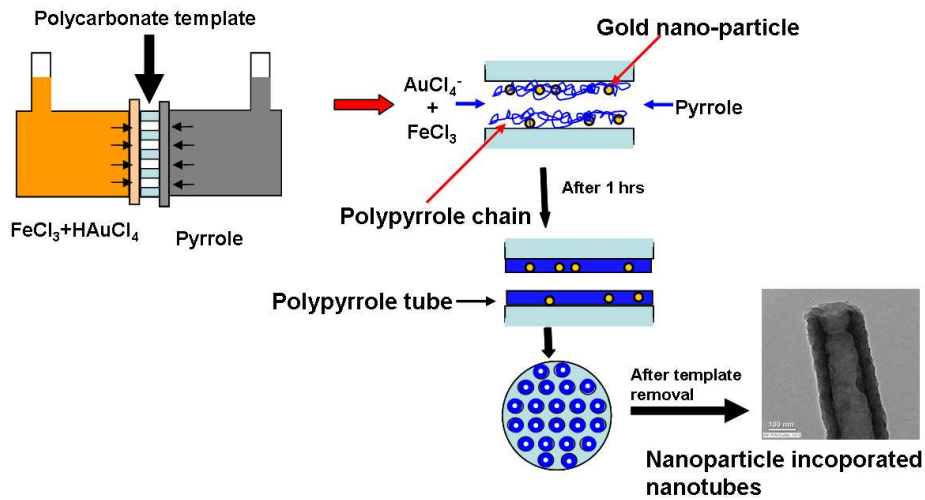


Figure 2.1: Schematic one step template based technique used for the synthesis of gold-polypyrrole composite nanotubes.

vealed by using a suitable chemical agent (like NaOH, HF etc) that selectively etches the latent track to create a hollow channel keeping the remaining part untouched [98]. Using this porous polycarbonate membrane as template gold-polypyrrole composite nanotubes and polypyrrole nanotubes has synthesized which will be presented in next subsection.

After the synthesis of nanowires inside the porous membrane, it is necessary to remove the template to get the individual nanowires. Polycarbonate membrane can be dissolved using Chloroform, N-methyl-2 pyrrolidine, Methylene chloride etc. These solvents have no apparent effect on the doping level of conducting polymer nanowires that keeps properties of nanowires intact.

2.2.1 Synthesis of gold-polypyrrole composite nanotube in chemical route

The growth method used here uses a salt that dissociates into a metallic anion to act as an oxidizing agent for promoting polymerization reaction. The

formation of gold-polypyrrole composite [99] occurs in the pores of the membrane and this process helps to disperse gold ions through out the nanotubes, homogeneously. In this growth technique, the membrane is placed between a two compartment glass cell with rubber O-ring and clip. One compartment is filled with 0.1 M monomer, while in the other compartment 0.5 M ferric chloride and 3 mM chlorauric acid solution is taken in volumetric ratio of 1 : 1 (refer in Figure 2.1). When these chemicals are allowed to mix through the nanopores of the membrane the polymerization reaction starts immediately and within few minutes polycarbonate membrane becomes black. The chlorine (Cl^-) and metal chloride anion ($AuCl_4^-$) react in the pores of the template with pyrrole monomer. Pyrrole reacting with ferric chloride produces polypyrrole which first get deposited on the surface of the pore walls [100] to form the nanotube. The reaction of chloroauric acid and Pyrrole produces gold [99, 101] that get embedded within the tube wall. The details of the reaction is presented in Figure 2.2. During polymerization reaction pyrrole monomer get oxidized and linked with each other to form dimer. Aging dimer get oxidized to form trimer and this process goes on, which results polypyrrole. Chloroauric acid contains gold-chloride ion which reacts with polypyrrole and gold get deposited [99]. The thickness of the membrane used was about $10 \mu\text{m}$ that determines the length of the tubes formed. We have observed that though chloroauric acid alone reacts violently with pyrrole monomer in a pot but this reaction does not occur properly in the pores of the polycarbonate membrane to form polypyrrole nanotubes. Gold incorporated polypyrrole sedimentation primarily occur in the compartment containing Pyrrole monomer. Mixture of chloroauric acid and ferric chloride in certain molar ratio is required to form nanotubes of gold-polypyrrole composite inside the pores of the polycarbonate membrane. As chloroauric acid is a

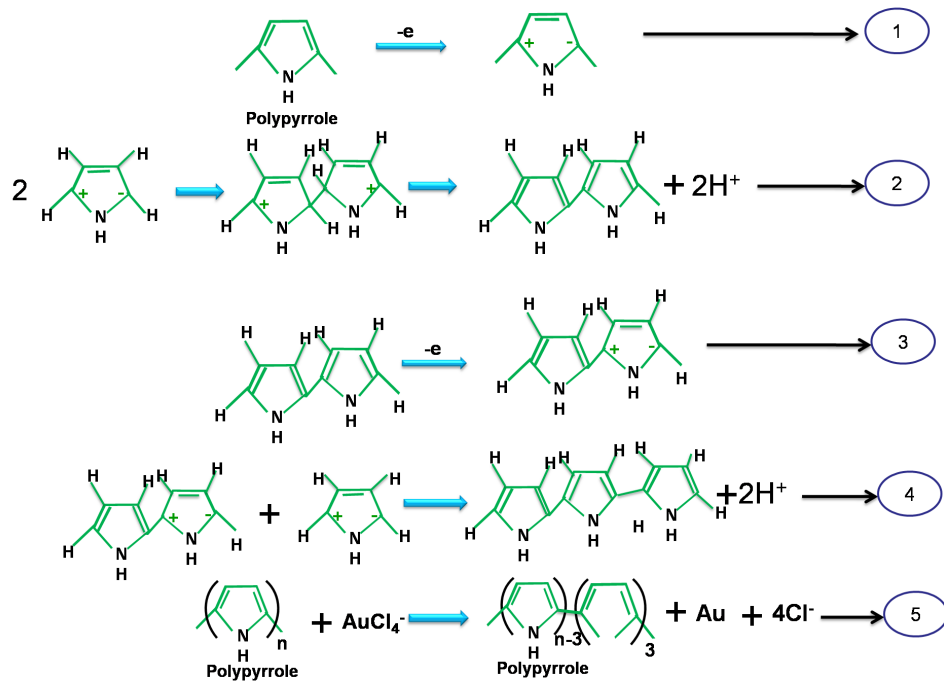


Figure 2.2: Reaction mechanism of chloroauric acid and pyrrole monomer. Pyrrole monomer get oxidized by leaving one electron, two such oxidized ring formed dimer then this goes on repeatedly and polypyrrole forms. Due to the reaction with chloroauric acid polypyrrole further oxidization occurs and gold get deposited. Reaction of ferric chloride and pyrrole described well by steps, from 1-4

strong oxidizing agent and can oxidize pyrrole quickly compared to ferric chloride, possible reason for this observation is that chloroauric acid diffuses through the pores and reacts with Pyrrole monomer before it can diffuse through the pores of the membrane and reaction occurs outside the template. If molar concentration of the chloroauric acid is reduced to have the reaction in the pores of the membrane, we found that lack of oxidizing reagent prohibit good tube formation. Only the reaction of a mixture of ferric chloride and chloroauric acid with higher ferric chloride molar concentration produce the composite nanotubes reported here (refer the schematic Figure 2.1).

2.2.2 Polypyrrole nanotube & chemical route

During the synthesis of polypyrrole nanotube we have used the same template based technique described above. But, we have used only ferric chloride ($FeCl_3$) as a oxidizing agent of pyrrole. So, the reaction occurs between $FeCl_3$ and pyrrole to form polypyrrole nanotubes.

2.3.0 Characterization

2.3.1 Scanning Electron Microscopy (SEM)

Scanning electron microscope basically consists of few basic components of electron optics. Electrons are generated from the Field emission gun and then accelerated by high voltage (1-30 keV) towards the sample through some electromagnetic lenses. The purpose of these electromagnetic lenses is to provide focused electron beam ($< 10\text{nm}$). In the beam path there are deflecting plates which are for the purpose of electron-beam deflection. The electron beam, when fallen on the sample, generates secondary electrons which are collected by detectors. Detectors collect signal and sent to the computer after amplification. In order to get for selected zone of the sample, the electron beam rasters the sample. The emitted signals from the sample are Secondary electrons (SE) and backscattered electrons (BSE). Depending upon the material and imaging purpose, we collect either SE or BSE using corresponding detector. One of the schematic picture of the SEM is shown in Figure 2.3, where different parts of SEM are indicated In order to find the shape of polymer nanocomposite inside the pores of polycarbonate membrane we have used SEM. For the imaging of these nanotubes we first remove the polycarbonate from one face of the mem-

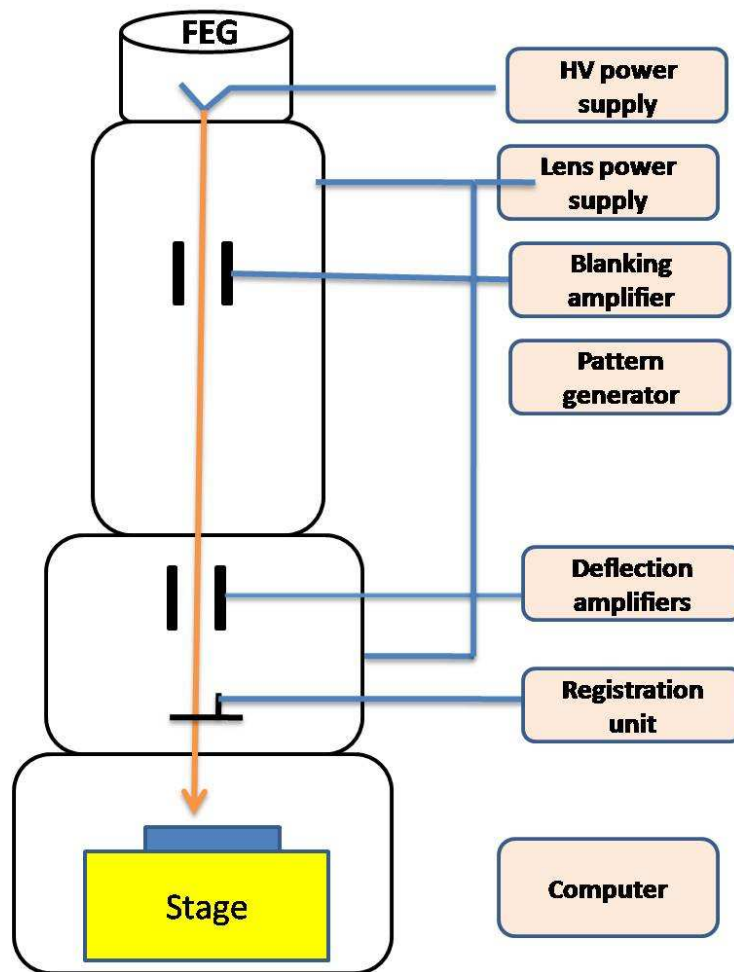


Figure 2.3: *Schematic of the Scanning Electron Microscope*

brane using Chloroform as all these polypyrrole nanotubes are embedded well inside the polycarbonate membrane. The removal of 90% of polycarbonate from one face of the membrane results in the exposure of embedded nanotubes, which is shown clearly in Figure 2.4a,b,c. Figure 2.4c is showing the side view of grown nanotubes, from which it is clear that nanotubes are parallel and are not intercalated. As it is clear that from 2.4b and 2.4d that the gold-polypyrrole nano-composite formed nanotubes. Scanning electron micrograph does not provide any clear signature of gold.

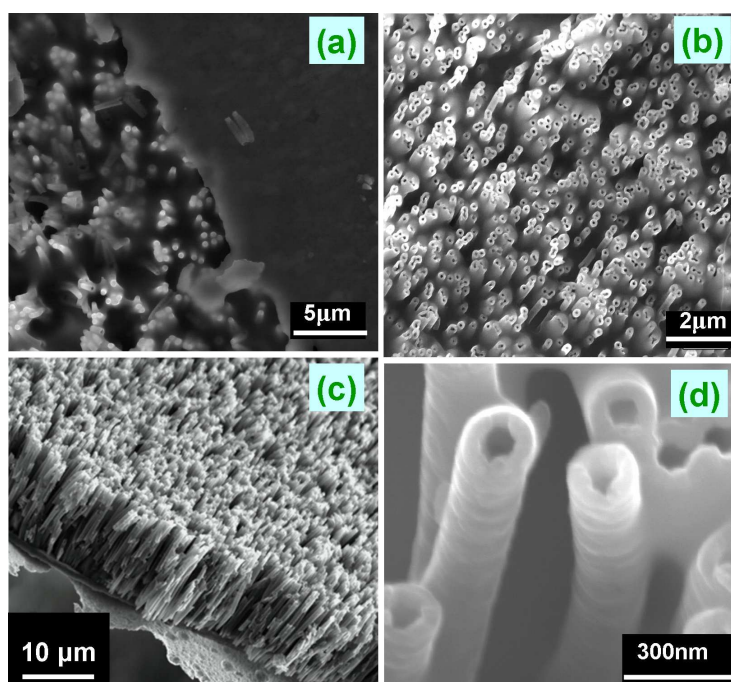


Figure 2.4: *Schematic one step template based technique used for the synthesis of gold-polypyrrole composite nanotube*

2.3.2 Transmission Electron Microscopy (TEM)

The transmission electron microscope (TEM) operates on same basic principles as the light microscope, but only electrons instead of light. The visibility of an object in light microscope is limited by its wavelength. On the other hand TEMs use electrons as "light source" having much lower wavelength which makes it possible to get resolution, thousand times better than with a light microscope. As a result we can see objects to the order of a few angstrom (10^{-10} m) in TEM.

An "electron source" at the top of the microscope emit electrons that travel through vacuum in the column of the microscope. Instead of glass lenses focusing the light in the light microscope, the TEM uses electromagnetic lenses to focus the electrons into a very thin beam. The electron beam then trav-

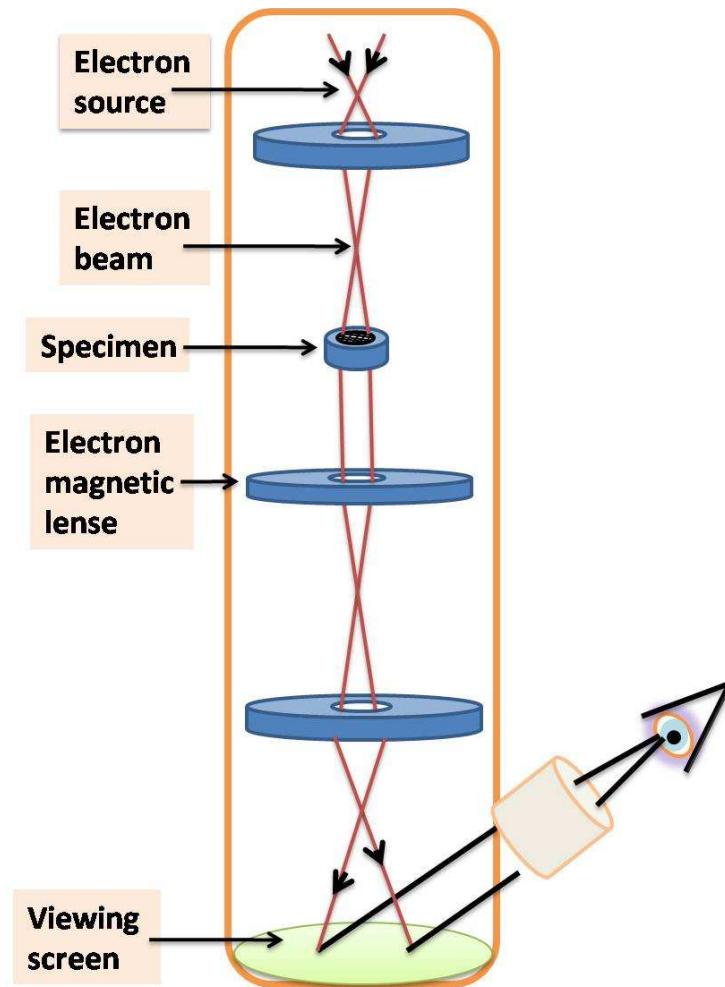


Figure 2.5: *Schematic of the Transmission Electron Microscope*

els through the specimen we want to study. Depending on the density of the material present, some of the electrons are scattered and disappeared from the beam. At the bottom of the microscope the unscattered electrons hit a fluorescent screen, which gives rise to a "shadow image" of the specimen with its different parts displayed in varied darkness according to their density. The image can be studied directly by the operator or photographed with a camera. To examine the gold and additionally morphology and structure inside the polypyrrole nanotube we have done TEM utilizing FEI, Tecnai G2 20, S-TWIN

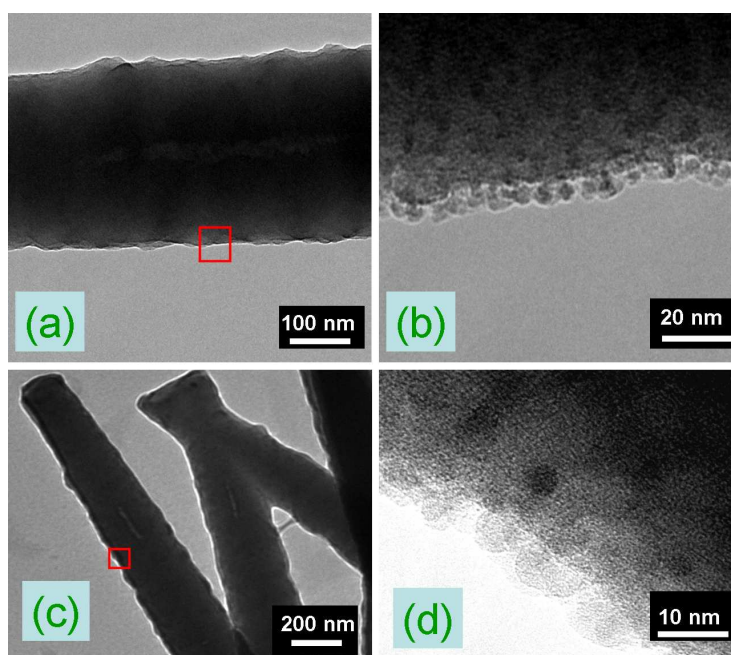


Figure 2.6: (a), (c) Low magnification image of gold incorporated nanotube and (b), (d) corresponding high magnification images. In the high magnification image few dark spot is visible which are due to embedded gold nanoparticle.

magnifying lens working at 200 kv, outfitted with a GATAN CCD. For TEM analysis the created nanotubes were take out from the pores by dissolving the membrane in chloroform, then it was sonicated and likewise a drop of it was put on a carbon coated copper grid for TEM study. As it is shown in the figure that from the low magnification images (Figure 2.6 a, 2.6c) as well as corresponding high magnification images (Figure 2.6 b, 2.6d) the presence of gold is not so clear. In Figure 2.6b and Figure 2.6d only few dark contrast particle is visible. The visibility of any crystalline plane was impossible in further high magnification image as these particles are embedded inside the polypyrrole matrix. In order the find the structure of nanoparticles we have exposed the nanotubes for several minutes under focused electron beam and drilled the nanotubes to find the clearer cross-sectional view. Figure 2.7a and Figure 2.7b showing the view of the nanotubes before and after drilling respectively. In Figure 2.7b the clear

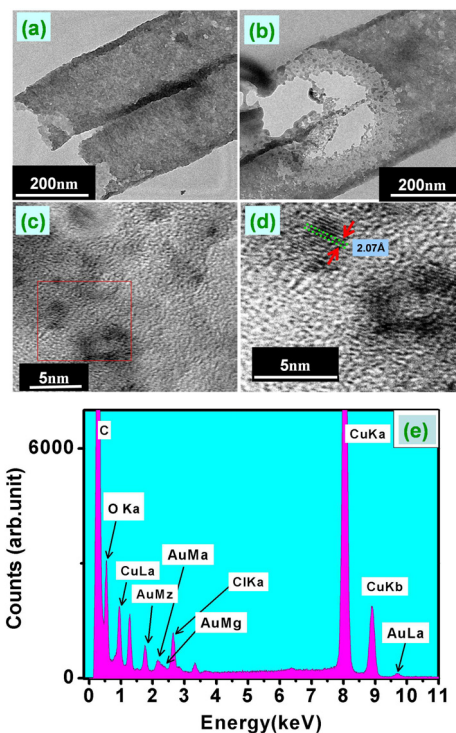


Figure 2.7: (a) Low magnification TEM image; (b) The part of nanotube which is exposed to the electron beam of 200 keV for several minutes; (c) High-magnification image of the beam exposed part of the nanotube showing nanocrystalline particles (d) HRTEM images showing crystal plane of Au; (e) EDX from single tube showing existence of gold.

cross-section of the nanotubes is shown. In Figure 2.7c and d we have shown the magnified micrograph of the cross-section part where gold nanoparticles are clearly visible. From the above study we are sure that incorporated gold nanoparticles are uniformly embedded inside polypyrrole matrix. We have also done the Energy Dispersive X-ray (EDX) spectroscopy measurement in TEM. A representative EDX spectra is shown in Figure 2.7e, which again confirming the presence of gold in polypyrrole matrix.

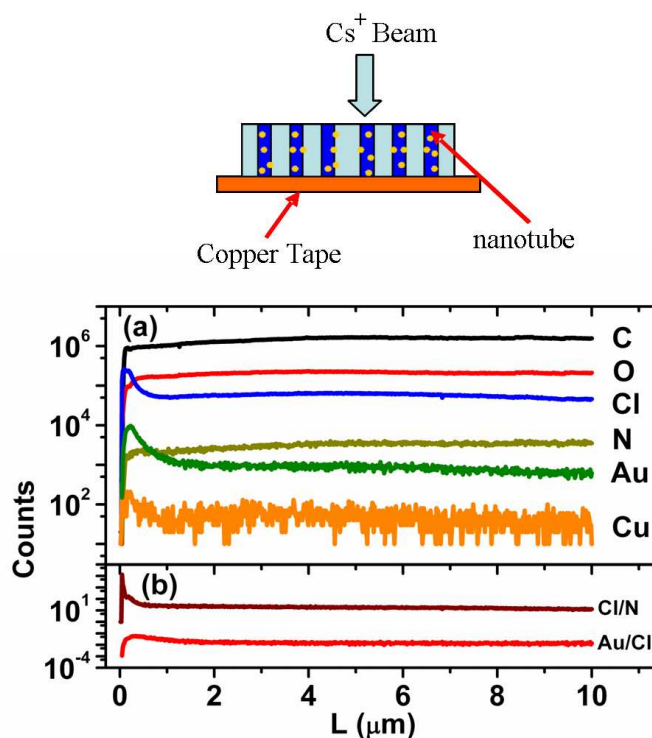


Figure 2.8: The membrane containing gold-polypyrrole composite nanotube is attached on a conducting silicon using copper tape. Using Cs^+ ion beam it is bombarded. (a) Showing the counts of different composition element along the length of the nanotube, (b) showing the ratio of chlorine to nitrogen and gold to chlorine is constant along the length of the nanotube

2.3.3 Secondary Ion Mass Spectroscopy (SIMS)

Secondary Ion Mass Spectroscopy (SIMS) is a very powerful surface analysis technique offering high-sensitivity quantitative elemental analysis with detection limits in the ppm-ppb range. With SIMS, the surface of a sample is bombarded with a focussed beam of primary ions and the impact of the ions with the target atoms eventually leads to the sputtering of the surface atoms or molecules. A small fraction of the sputtered ionized (positive or negative) species, produces secondary ions in the SIMS process. The energy and mass analysis of these secondary ions forms the basic of SIMS. The energy analysis

is done by a sector electrostatic energy analyzer and the mass analysis is done by a suitable mass spectrometer. The mass-spectrometer uses electrostatic and magnetic fields to separate the ions according to their mass-to-charge ratio. SIMS is destructive by its nature (sputtering of material) but can be applied to any type of material (insulators, semiconductors, metals) that can stay under ultra-high vacuum. SIMS can operate in static SIMS or dynamic SIMS modes. Static SIMS uses a pulsed primary ion beam of low current density to sputter material from sample resulting molecular as well as elemental characterization of the topmost monolayer. On the other hand, the main application of dynamic SIMS is the investigation of bulk composition or in depth distribution of trace elements present. Because of the high erosion rate in the dynamic SIMS compared to static SIMS, the detection sensitivity in dynamic SIMS is much higher than that in static SIMS. We have used the SIMS instrument (Hiden Analytical Limited, UK) of our laboratory for all the measurements (dynamic mode). The sample is bombarded with cesium ion (Cs^+) at 5 keV that sputter the constituents material from the sample and the obtained sputtered materials were analyzed using mass spectrometer to identify constituent. For the SIMS measurement, a piece of polycarbonate membrane having nanotubes (diameter 200 nm) was mounted with copper tape in such a way that we can get compositional information along the length (depth of the membrane) of the tubes. It is known that Polycarbonate membrane is composed of Carbon (C), Oxygen (O), Hydrogen (H) and polypyrrole is composed of C, N, H, Cl (dopant). Chlorine ion acts as doping as well as oxidizing agent in polypyrrole formation. The SIMS data (Figure 2.8 a) shows that count of N and Cl are constant over the length of nanotubes and Figure 2.8b shows that the ratio of Cl/N is constant, which implies polymerization and doping occurs uniformly along the length of

nanotube [102]. However the surface of the membrane which was facing the compartment containing Ferric chloride and Chloroauric acid during chemical reaction, shows higher value of Cl and Au in the profile as reported earlier for Polypyrrole nanowires [102]. Figure 2.8a showing the steady count of gold apart from this end of tube indicating that the gold is homogeneously dispersed along the length of the nanotubes. The Figure 2.8b clearly show Au/Cl ratio remain constant over entire length of the tubes as the gold profile follow the Chlorine profile.

2.3.4 Magnetron Sputtering

For the deposition of metallic electrodes to connect the polymer nanowires, we have used dc magnetron sputtering in our laboratory. In the dc-sputtering, a negative potential (\sim hundred Volts) is applied to the target. To enable the ignition of a plasma, usually argon is fed into the chamber up to a pressure between $1 \times 10^{-2} - 3 \times 10^{-3}$ mbar. By natural cosmic radiation there are always some ionized Ar^+ ions available. The Ar^+ -ions are accelerated towards the target which not only sputter the material but also produces secondary electrons. These electrons cause a further ionization of the gas. To increase the ionization rate by emitted secondary electrons even further, a ring magnet below the target is used in the magnetron sputtering. The electrons in its field are trapped in cycloids and circulate over the target surface. By the longer dwell time in the gas they cause a higher ionization probability and hence form a plasma ignition at pressures, which can be up to one hundred times smaller than that for conventional sputtering. Therefore, higher deposition rates can be realized. On the other hand, less collisions occur for the sputtered material

on the way to the substrate because of the lower pressure and hence the kinetic energy at the impact on the substrate is higher. The electron density and the number of generated ions become maximum in the region where the magnetic field is parallel to the substrate surface. The highest sputter yield happens on the target area right below this region. An erosion zone is formed which follows the form of the magnetic field. Thus large number of Ar^+ ions of the plasma are accelerated towards the target consisting of the material to be deposited and material is sputtered from the target and afterwards deposited on a substrate in the vicinity. The process is realized in a closed recipient which is pumped down to a vacuum base pressure before deposition starts. We have used a Pfeiffer made DC/RF magnetron sputtering unit (PLS 500). The main chamber was pumped out by a turbo molecular pump followed by a rotary pump. The base pressure was better than 1×10^{-6} mbar. There were two dc source and one rf source. High purity sputter sources (target) of 50 mm diameter and few mm thickness were used. The dc power can be varied from 10 -500 watt. Argon gas flow is controlled by a MKS mass flow controller. We have made several sample holder so that deposition of metals should be done at certain angle ($\sim 30^\circ$). We prefer metal deposition at angular configuration on the both sides of the template having nanotubes. Because this step removes the possibility of entering metals deep inside the nanowires/nanotubes.

2.3.5 Thermal evaporator [Designed in Lab]

We have used the Lab-designed evaporator during electron-beam lithography for the deposition of nano-pattern. Thermal vacuum deposition is one method for fabricating thin films under a high vacuum environment also ad-

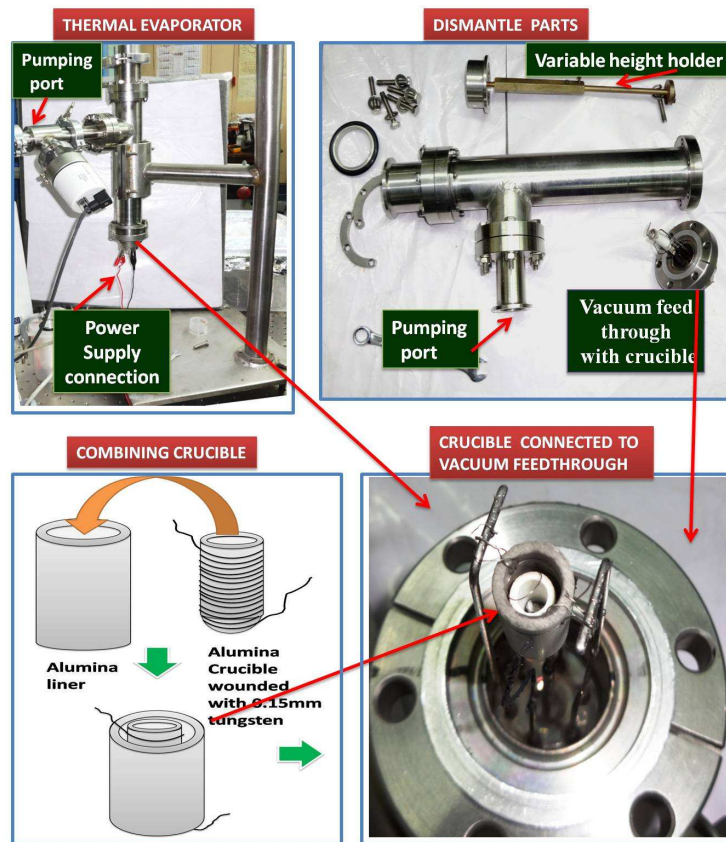


Figure 2.9: Showing different parts of the thermal evaporator

dressed as "thermal evaporation method". With this method, an electron beam (e-beam) or resistive heating is usually used to evaporate the desired material inside the vacuum coating chamber. We have used here resistive heating method. The material to be deposited is loaded into a heated container called a crucible. The crucible is resistively heated by applying a large current. As the material in the crucible becomes hot it gives off a vapor whose atoms travel in straight lines until they strike a surface where they accumulate as a film. The basic facility of thermal evaporation over sputtering is that the evaporated material is deposited on the target substrate at low energy (eV) as a result the penetration of deposited material on the targeted surface is small. The directionality of the evaporated material is better which results in low step coverage.

Table 2.1: Comparison between Magnetron Sputtering and Thermal evaporation

Sputtering	Thermal Evaporation
High energy atoms or ions (1 - 10 eV) 1 > denser film 2 > smaller grain size 3 > better adhesion	Low energy atoms (~ 0.1 eV)
Low vacuum 1 > poor directionality, better step coverage 2 > gas atoms implanted in the film	High vacuum 1 > directional, good-for lift-off 2 > lower impurity
Parallel plate source better uniformity	Point source poor uniformity
All component sputtered with same rate 1 > maintain stoichiometry	Component evaporate at different rate 1 > poor stoichiometry

This property is very useful during nano-patterning of a chip or during shadow masking.

Design

During making this thermal evaporator we have used the design of Knudsen-cell. The crucible is made of high purity alumina which is wound with 0.15 mm tungsten wire upto 30 turns in 1 cm length. The windings are denser towards the top of the crucible. This crucible is then jacketed by a alumina liner which prevent the loss of heat. Electrical connections were done using a vacuum feed-through, as shown in the Figure 2.9. There is a variable height sample holer for changing the distance between the sample and crucible. We have put one thermocouple in the sample holder just beneath the sample holding clip which used for the purpose of monitoring the temperature of the sample. This chamber can sustain the vacuum upto 10^{-6} mbar. A clear picture of the different parts of the evaporator is shown in Figure 2.9.

2.4.0 Electron beam Lithography

Electron beam lithography means to writing pattern on a substrate which is coated with a electron beam sensitive layer. By combining the scanning of electron beam and the high precision motion of a stage, it becomes possible to fabricate design at nanometer resolution.

2.4.1 Types of e-beam resist

The energy (5-25 keV) of the incident electrons in Scanning Electron Microscope is much higher than the energy associated with chemical bonds of various materials. Most such materials are polymers comprising long -chain molecules which changes their properties, on irradiation. There are mainly two type of resist; positive e-beam resist and negative e-beam resists.

Positive resist

When e-beam irradiated on polymer, the polymer are breaks (cross linked bonds) into smaller part which solvable in certain solution and the rest of the film remains intact. Few of the positive resists are

1. Poly (methacrylate)
2. Crosslinked methacrylates
3. Polyoleh sulphones

Negative resist

When e-beam irradiated on polymer, the cross-linking in the polymer increases

as a result the solubility in certain solvent decreases rapidly. So, after irradiation when we dipped it in certain solvent the whole film of the resists becomes wash out but only those irradiated portions of the films are remains intact. Negative e-beam resist include mainly, materials with the following chemical groups: *Vinyl* – $CH = CH_2$, *Allyl* – $CH = CH - CH_2$, *EPOXY* – $HC - CH-$.

2.4.2 Pattern Designing

Although electron beam lithography tools are capable of forming extremely fine probes, things become more complex when the electrons hit the workpiece. As the electrons penetrate the resist, they experience many small angle scattering events (forward scattering), which tend to broaden the initial beam diameter. As the electrons penetrate through the resist into the substrate, many of them will experience large angle scattering events (backscattering). The backscattered electrons cause the proximity effect, where the dose of a pattern feature is affected by electrons scattering from other features nearby. During this process the electrons are continuously slowing down, producing a cascade of low energy electrons called secondary electrons with energies from 2 to 50 eV. They are responsible for the exposure of the bulk resist. Since their range in resist is only a few nanometers, they contribute little to the proximity effect. Instead of that, the net result can be considered to be an effective widening of the beam diameter by roughly 10 nm. This largely accounts for the minimum practical resolution of 20 nm observed in the highest resolution electron beam systems. In basic SEM conversion systems the proximity effect caused by the backscattered electrons limits the resolution ~ 100 nm. This resolution level can be increased using some sort of dose correction method. The

main effect of proximity effect is that small features are exposed less than the larger features, which causes significant distortion in very small features (that is also the reason why the exposition rate may depend on pattern geometry and size). The simplest dose correction method, is the use of double layer e-resist, but this only works for quite large features ($1 \mu\text{m}$). The other dose correction methods usually consist of calculating the cumulative exposition rate that a feature receives directly from the beam and also from other features, and then compensating for the excess dose by adapting the beam current (from feature to feature), the speed with which the beam scans over the sample, or the shape of the drawn features.

2.4.3 Connecting single polypyrrole nanotube for electronic transport measurements (RECIPE)

In order to make connection from single polypyrrole nanotube for electronic transport measurement we have used the electron-beam-lithography (EBL). The total structure is fabricated on a silicon-di-oxide coated silicon substrate. In Figure 2.10 we have presented the overall picture of the chip on which single nanotube is connected. The whole process is basically divided in four steps

- FABRICATION OF BIGGER ELECTRODES.
- FABRICATION OF SMALLER ELECTRODES AND MARKERS.
- DISPERSION OF POLYPYRROLE NANOTUBES.
- MAKING CONNECTIONS OF SINGLE POLYPYRROLE NANOTUBE.

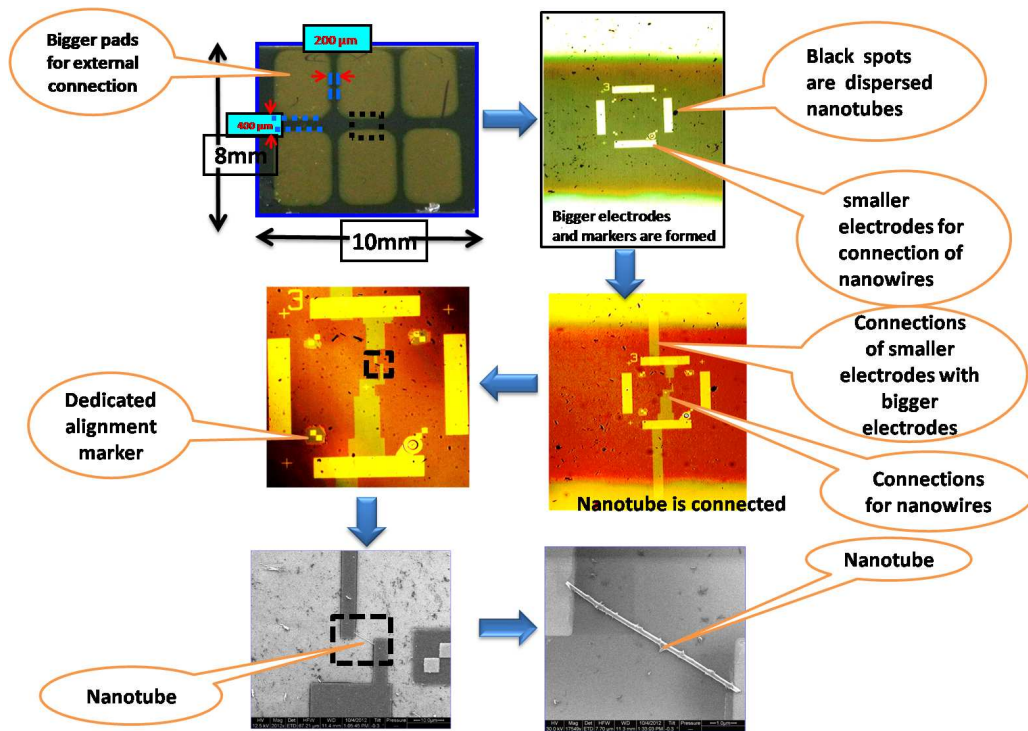


Figure 2.10: *Contacted nanotube at different magnification*

CLEANING

Here we have used 200 nm SiO_2 coated degenerate silicon (Si) as basic substrate for chip fabrication. It is cleaned with isopropyl alcohol, acetone and Millipore water respectively. After cleaning it is dried by flowing dry nitrogen gas.

FABRICATION OF BIGGER ELECTRODES

Using the mask of stainless-steel, we have deposited bigger electrodes from which we will take out final connections for measurements. After masking, we deposit 10 nm chromium and then 200 nm gold in high vacuum using magnetron sputtering. In this process we deposit six electrodes where size of the each pad is 4 mm X 3 mm. The gap between two opposite pads is 400 μm , as shown in Figure 2.11.

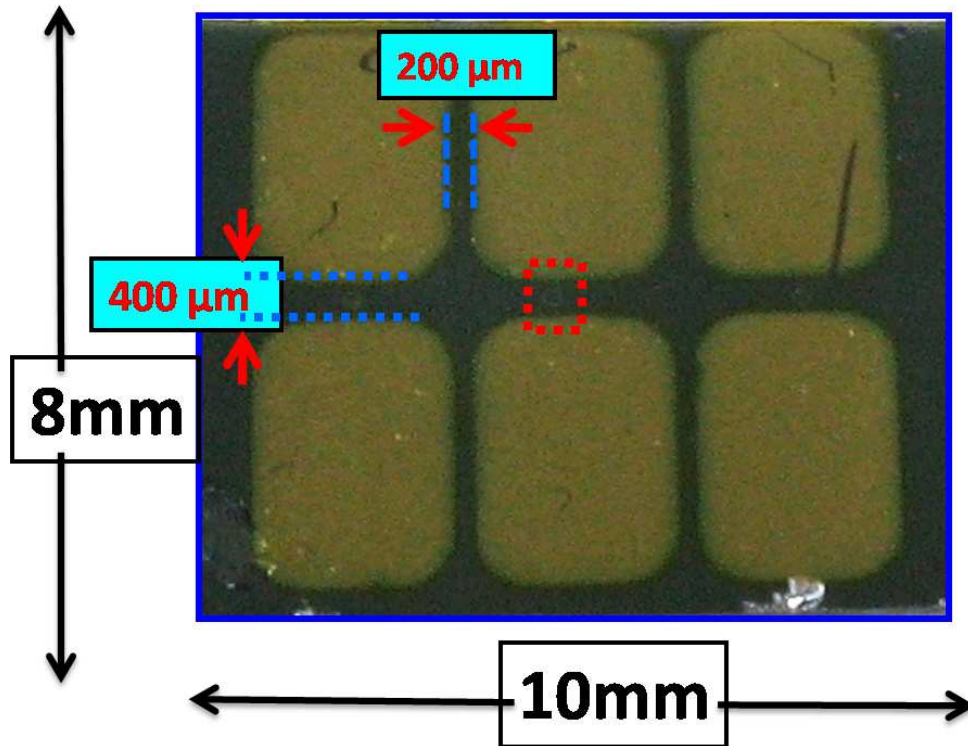


Figure 2.11: *Fabricated bigger gold electrode on silicon-di-oxide coated silicon substrate*

FABRICATION OF SMALLER ELECTRODES AND MARKERS

1. **Spin Coating:** We have used poly-methyl methacrylate acetate (PMMA-950K, 4% in anisole) as positive e-beam resist. Spin coat this e-beam resist at 1200rpm for 60sec. We find 400nm film has deposited.
2. **Annealing:** After spin coating the substrate was annealed at 180 °C for 2min on hot plate and after that kept it at 30 °C for 24hrs.
3. **Writing:** Within SEM, draw the marker and smaller electrodes (20 μm X 10 μm) on the PMMA coated substrate using e-beam at 30 keV energy and beam dose of 180 μC/cm².

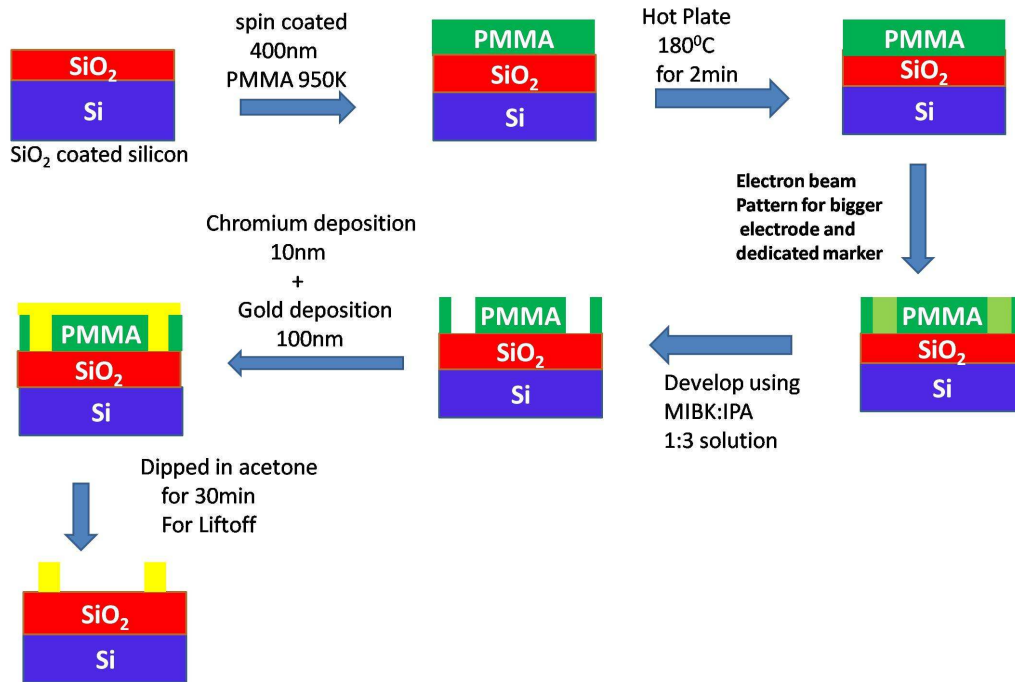


Figure 2.12: Showing different steps for fabrication of smaller electrode and dedicated marker, we followed

4. **Develop:** After e-beam writing we develop the smaller electrode pattern by dipping it in a solution of MIBK: IPA (1 : 3) for 30 sec and after rinsing in Millipore water dry it by blowing dry nitrogen. As a result, we find that the exposed portions of the film in the e-beam are removed.
5. **Metal deposition:** Using sputtering we deposit first 10 nm chromium as adhesive layer, then deposit 200 nm gold on it.
6. **Final development[Lift-off]:** After metal deposition dip it in acetone for 20 min to liftoff the remaining metal coated PMMA. Then dry it by Nitrogen gas flow, followed by step of rinsing the chip in Millipore water.

The above mentioned steps are shown schematically in Figure 2.12.

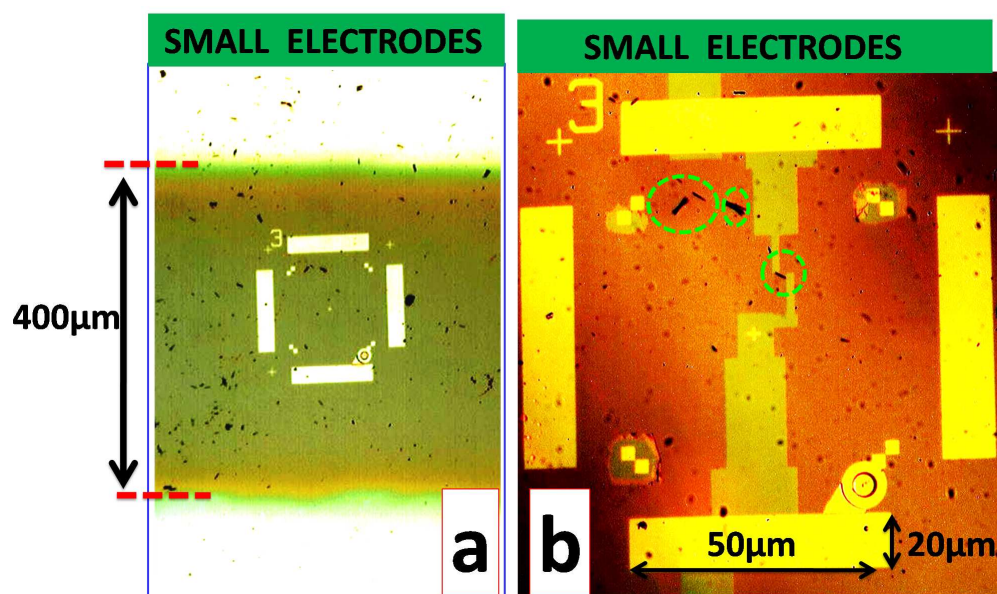


Figure 2.13: The image of the chip after dispersion of polypyrrole nanotubes where markers and smaller electrode are fabricated in the earlier step. Left one and right one are the low and high magnification images. Dark spots in image corresponds to the dispersed nanotubes, few of the clear nanotubes are marked by red dotted circle.

DISPERSION OF POLYPYRROLE NANOTUBES

The gold incorporated polypyrrole nanotubes grown within the pores of the polycarbonate membrane, as mentioned earlier section. In order to make single nanotubes connection we have to separate these nanotubes individually by dissolving it into chloroform. After dispersion of polypyrrole nanotubes in chloroform, sonicate the solution for 2hrs at 50 watt power of sonicator. Then drop cast the solution on the chip fabricated earlier. Using optical microscope several images were recorded after dispersion of nanotubes on the chip. One typical image is shown in Figure 2.13. In Figure 2.13a and a Figure 2.13b showing images at low magnification and high magnification respectively. All these black debris are single and bunch of nanotubes. Blue dotted circles in the magnified image

showing nanotubes. In the figure the bigger pad dimension is $50\ \mu\text{m} \times 20\ \mu\text{m}$. Four such pad is shown in Figure 2.13. Dedicated markers are consists of two $5\ \mu\text{m} \times 5\ \mu\text{m}$ square are connected at corner.

MAKING CONNECTIONS OF SINGLE POLYPYRROLE NANOTUBE

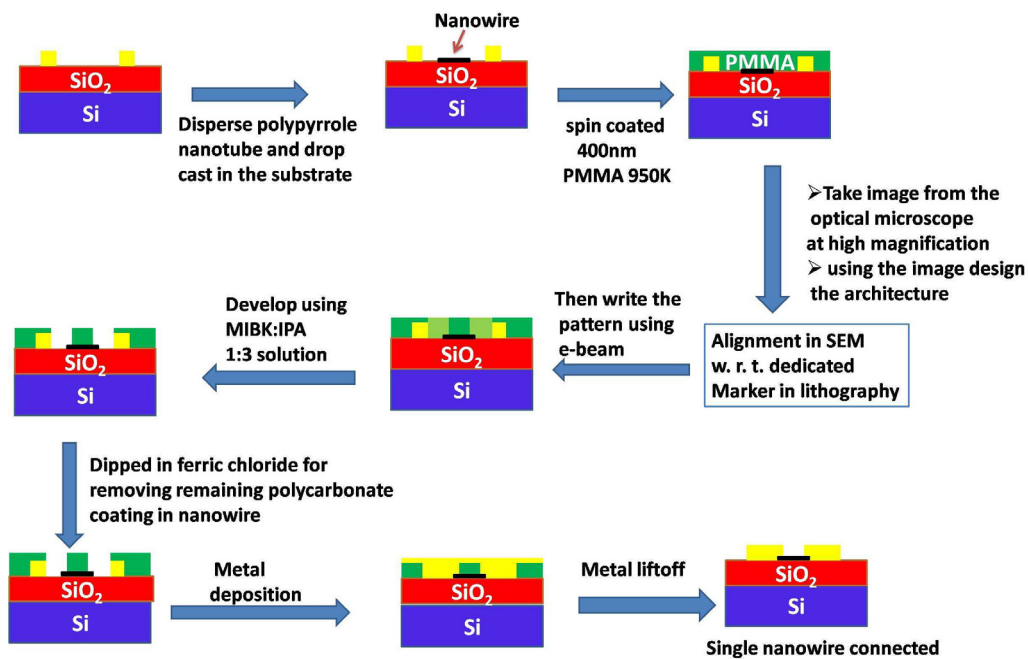


Figure 2.14: *Showing different steps to take connection from single nanotube, we followed*

1. Using Spin-coater grow 300 nm layer of PMMA950K on the earlier fabricated chip after dispersion of nanotubes.
2. Anneal for 2 min at 180°C and kept it at 30°C for 24 hrs.
3. Using optical microscope at 50X zoom capture a picture, where at least one nanotube is visible within the pattern (typical image is shown in Figure 2.13).

4. Then transfer the image in a computer and use Adobe Illustrator to draw a pattern. The purpose of this patterning is to draw the connecting path from both ends of the nanotube to two different connecting ($50\ \mu\text{m} \times 20\ \mu\text{m}$) pad. The major important point of this step is to accurately measure the length scale of the optical microscope image. For length calibration we use the known length of the dedicated marker.
5. Transfer the image in the lithography machine computer and load the sample in the lithography chamber.
6. First check the focusing of the beam using polystyrene ball which is at corners of the sample. Choose the proper dose and set the instrument. Then align the sample using dedicated markers. Finally, write the proper design to the sample for connecting single nanowire.
7. Then develop the sample using developer solution (MIBK:IPA 1:3) for 30 sec. Dry it by blowing dry nitrogen gas.
8. In order to remove the remaining polycarbonate coating which is on the surface of polypyrrole nanotube dip the chip in 0.5 M ferric chloride solution for 2 hrs. Then after cleaned with Millipore water and dried. Removal of this coating is very important in order to get good ohmic contact with nanotubes.
9. In order to have better ohmic contact Magnetron sputtering is used to deposit first 10 nm chromium and 150nm gold. [for ohmic contact preferred sputtering]
10. During the liftoff process dip the chip into acetone for 1hrs and after cleaning with Millipore water dried by dry nitrogen gas.

11. Perfection of connections are checked using optical microscope and electronic transport.

The schematic of this process is shown in Figure 2.14. Optical image and SEM image at different magnification of the chip after connecting the single nanotube, is shown in Figure 2.15.

Note: DO NOT EXPOSE THE BARE SAMPLE, ELECTRODES, NAN-

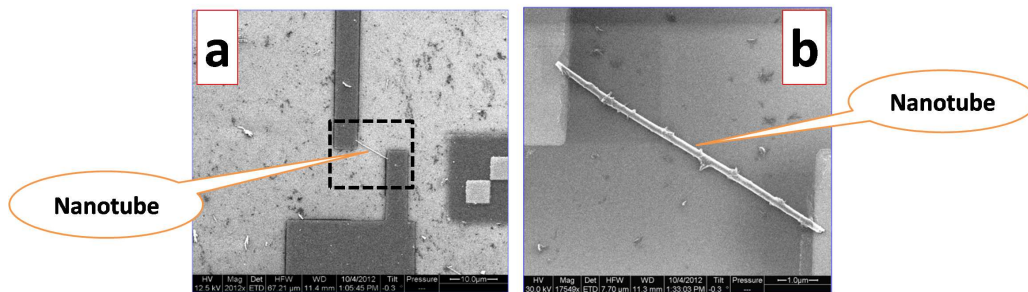


Figure 2.15: *Contacted nanotubes: (a) Lower magnification, (b) At higher magnification, where the deposited gold at one end of nanotube is visible.*

OTUBES TO THE ELECTRON BEAM. BECAUSE DURING VIEWING THE BARE SAMPLE WITH ELECTRON BEAM THERE WILL BE DEPOSITION OF CARBON AND CREATION OF DEFECTS, AS THE BEAM ENERGY IS SUFFICIENTLY HIGH. SO BEFORE DOING ELECTRONIC TRANSPORT MEASUREMENT, IT IS RECOMMENDED NOT TO VIEW BARE CHIP OR SAMPLE IN SEM.

2.5.0 Connections of multiple nanotubes

As we mentioned earlier that nanotubes are formed within the polycarbonate membrane which makes each polypyrrole nanotubes parallel and insulated from each other. Each of these nanotubes are extended from one side of

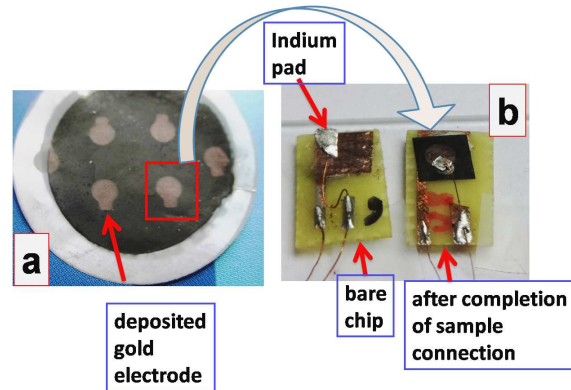


Figure 2.16: (a) Showing the deposited gold electrode on the surface of the membrane containing nanotubes, (b) after taking connections from the piece of membrane having connecting pads.

the membrane to other. This situation made feasible the measurement of electronic transport properties of these nanotubes without separating them from the membrane. For this reason we deposit the gold-electrode on both sides of the membrane containing nano-composite nanotubes, as shown in the left of Figure 2.16. Then we cut the membrane properly into rectangular pieces (4 mm X 4 mm) and glued it with the connector chip (prefabricated electrodes and connections) using silver paint, as shown in right figure of Figure 2.16. For the connection from the front electrode surface of the sample, we have used indium pad connected with thin copper wire and attach it on the top surface of the sample using silver paint. Then we can easily takeout two or four connections from the chip for electronic transport measurement.

2.6.0 Low Temperature Measurements

We have used several set ups to measure low temperature dc and ac transport properties of our samples in the temperature range 1.7 to 300 K and in presence of magnetic field up to 7 tesla. Low temperature measurements were

done in a liquid helium cryostat equipped with a 7 tesla superconducting magnet (Oxford-Spectromag). Some of the zero field measurements were done using various closed cycle refrigerator (CCR) operating in the temperature ranges 2 to 300 K (Advanced Research System), 4 to 300 K (Janis) and 10 K to 300 K (Janis). In these CCRs, temperature was monitored and controlled using a silicon diode temperature sensor and Lakeshore 340 or 331 temperature controller.

2.6.1 DC and AC measurement setup

a. Insert Design

For the low temperature measurements using liquid helium cryostat we have designed an insert (see Figure 2.17) to mount multiple samples. Provisions were made to place each sample in homogenous magnetic field, to rotate the samples without breaking vacuum (so that magnetic field can be applied in any direction), to measure the exact temperature of the samples (so that effect of sample heating during current flow can be precisely monitored). We have

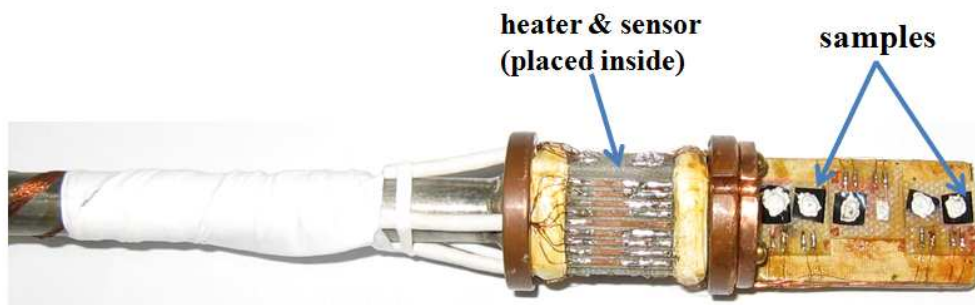


Figure 2.17: Home made insert used for the low temperature electronic transport properties measurements. Sample and position of heater and sensor has been shown.

used two 19 pin high vacuum electrical feed-through to connect the heater and sensor, rest 32 connections were left for connecting 8 samples (4-probe). The sample temperature was monitored using a cernox sensor placed near the sample. For heating we used a $50\ \Omega$ Manganin wire heater and connected it with Lakeshore 340 temperature controller. For various measurements we have used Keithley 2400 and 2602A source-measure unit, 2000 and 2001 Digital Multimeter, 6517A electrometer. Agilent 34420A nanovoltmeter, 33220A Function generator, E4980A precession LCR meter and 54622A 100 MHz oscilloscope. Stanford Research System Lock-in amplifier (SR-830), SR 760 FFT analyzer, SR 560 low noise voltage preamplifier, SR 570 low noise current preamplifier, Ithaco 1212 current amplifier, PAR 124A Lock-in amplifier.

For relatively low resistive sample we used Keithley 2400 source meter for current biasing and the voltage developed across the sample was measured using Nanovoltmeter or Digital Multimeter. For high resistive sample resistivity and I - V characteristics were measured using Electrometer or with the help of low noise current preamplifier. Before any high resistive measurement, the instruments performance was checked by choosing suitable resistance as a sample. One such I - V characteristics for $1\ G\Omega$ for $\pm 10\ mV$ bias has been shown in Figure 2.18. The measurement has been done by supplying voltage from the source meter or using the source of electrometer and the current flowing through the circuit is fed to the SR 570 low noise current preamplifier and the output voltage was measured using Nanovoltmeter or Digital multimeter. Required averaging has been done to minimize the effect of noise. Differential conductance vs. voltage (dI/dV - V) measurements were done by using SR 830 Lock-in amplifier, SR 570 low noise current preamplifier and Agilent 33220A Function Generator. For this measurement a small amplitude ac voltage is

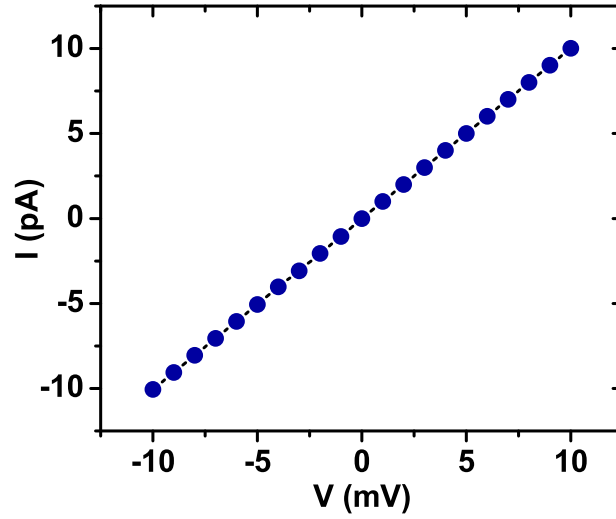


Figure 2.18: I - V characteristics of $1\text{ G}\Omega$ resistance (symbols are the data point).

added to the dc bias voltage using Function generator and the current response was detected by Lock-in amplifier at the same frequency of the ac voltage after amplifying it by SR 570 current amplifier. In presence of small amplitude ac bias the resultant current can be expressed as

$$I(V_0 + V_{ac} \cos(\omega t)) = I(V_0) + (dI/dV)V_{ac} \cos(\omega t) + 1/2(d^2I/dV^2)V_{ac}^2 \cos^2(\omega t) + \dots$$

where V_0 is the dc bias V_{ac} is the amplitude of ac bias having frequency ω . From the above equation we see that current response corresponding to ω is proportional to dI/dV . With the help of Lock-in amplifier we can easily detect the signal corresponding to ω and by varying the dc level we get a complete scan of dI/dV vs. V .

b. Current Bias low noise Magnetoresistance measurement set up

This circuit shown in Figure 2.19 is useful when the change of magnetore-

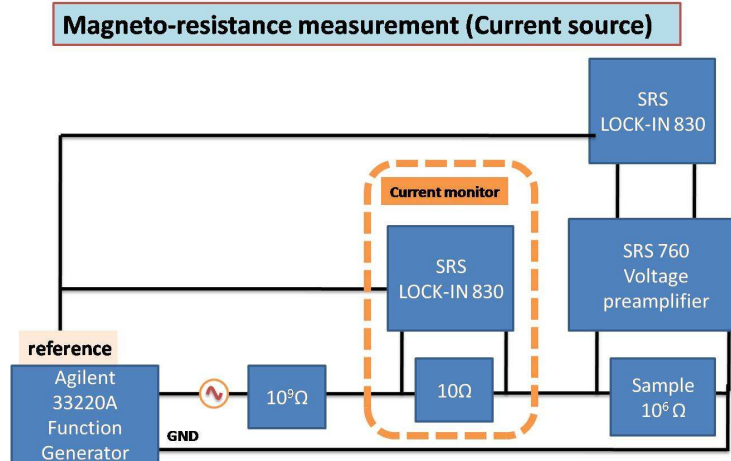


Figure 2.19: *Low noise magnetoresistance measurement .*

sistance is smaller compared to the resistance of the sample. For the measurement of low-noise magnetoresistance we have used two SR 830 Lock-in amplifier, SR 560 low noise voltage preamplifier and Agilent 33220A Function Generator. For this measurement a small amplitude ac voltage is added to the dc bias voltage using Function generator which is applied across the sample through a high series resistance (10^9 Ohm). The purpose of using high series resistance is to use the Function-generator as current source. The voltage across the sample is first amplified (optimized gain) using the voltage amplifier and the voltage is then measured using SR-830 which is locked at frequency same as the source ac voltage. Our sample resistance is (10^6). In order to constantly monitor the current in the circuit we have used a low noise 10Ω calibrated resistor in series with the circuit. The voltage across the standard resistor was monitored directly using another SR 830.

2.6.2 Dielectric Measurement

Dielectric constant of the sample was measured using Novocontrol Alfa-A analyzer. The low temperature dielectric measurements, have been done using specially designed insert. For the wiring of the insert we have used Lakeshore cryo-coaxial cable. During the measurement we have taken care about any inducting or capacitive effect coming from wirings. Before each measurement cycle we used to perform "short circuit", "open circuit" and "standard impedance" calibration. The other details are presented in Chapter 4.

2.6.3 Data acquisition

All the instruments were interfaced with a computer via GPIB interface. Due to the absence of IEEE port, out put of the PAR 124A Lock-in amplifier is feed to a Digital multimeter (Keithley 2000 or 2001) which is then interfaced with computer to record the data. LABVIEW (National Instruments Corp., Austin, TX) software has been used for data acquisition. Several programmes were written for the measurements of current-voltage, resistance-temperature, capacitance-voltage, capacitance-frequency, differential conductance-voltage, relaxation characteristics. In each programmes we have kept several flexibility for choosing suitable time delay, averaging, scan direction etc. To minimize the programming time we have made several sub-VI (virtual instrument) for the scan direction, averaging etc and use them directly to make a complete programme.

We have interfaced Novocontrol alfa-A analyzer using IEEE GPIB. But all the acquisition has been operated using WinDETA software. Dielectric data analysis was carried out using programmes written in mathematica.

2.7.0 X-ray (Synchrotron) measurement

We have used Synchrotron x-ray for hard x-ray photoemission study as well as to study the size and strain of the incorporated gold nanoparticles in nanotubes. We have studied the in-situ x-ray diffraction during the incorporation of gold nanoparticles in polypyrrole nanotubes. X-ray diffraction of the membrane containing gold-polypyrrole composite nanotubes in normal transmission geometry gives us the erroneous information due to surface deposited nanoparticles. In order to find the accurate information of the incorporated nanoparticles of the in-situ/ex-situ sample we have designed a cell. Details of the cell and measurement is presented in chapter 4. The details of the hard x-ray photoemission spectroscopy (HAXPES) is presented in the next chapter.